Electronic structures and thermoelectric properties of solid solutions $CuGa_{1-x}In_xTe_2$: A first-principles study*

Xue Li(薛 丽)[a], Xu Bin(徐 斌)[b], and Yi Lin(易 林)[a]†

[a] Department of Physics, Huazhong University of Science and Technology, Wuhan 430074, China

[b] Department of Mathematics and Information Sciences, North China Institute of Water Conservancy and Hydroelectric Power, Zhengzhou 450011, China

(Received 18 July 2013; revised manuscript received 10 September 2013; published online 24 January 2014)

The electronic structures of solid solutions $CuGa_{1-x}In_xTe_2$ are systematically investigated using the full-potential all-electron linearized augmented plane wave method. The calculated lattice parameters almost linearly increase with the increase of the In composition, which are in good agreement with the available experimental results. The calculated band structures with the modified Becke–Johnson potential show that all solid solutions are direct gap conductors. The band gap decreases linearly with In composition increasing. Based on the electronic structure calculated, we investigate the thermoelectric properties by the semi-classical Boltzmann transport theory. The results suggest that when Ga is replaced by In, the bipolar effect of Seebeck coefficient S becomes very obvious. The Seebeck coefficient even changes its sign from positive to negative for p-type doping at low carrier concentrations. The optimal p-type doping concentrations have been estimated based on the predicted maximum values of the power factor divided by the scattering time.

Keywords: $CuGa_{1-x}In_xTe_2$, electronic structures, thermoelectric properties, first-principles

PACS: 71.15.Mb, 71.15.Nc, 72.20.Pa **DOI:** 10.1088/1674-1056/23/3/037103

1. Introduction

Thermoelectric (TE) materials can convert waste heat into electric power and then reduce greenhouse gas emissions. The ability of a TE material is characterized by a dimensionless figure of merit $ZT = S^2\sigma T/(\kappa_e + \kappa_l)$,[1,2] where σ is the electrical conductivity, S is the Seebeck coefficient, T is the temperature, and κ_e and κ_l are the electronic and the lattice contributions to the thermal conductivity κ, respectively. Obtaining a TE material with a large ZT value is a challenging task, since a good TE material should satisfy some conflicting demands: high Seebeck coefficient and high electrical conductivity; yet low thermal conductivity.

The $CuXTe_2$ (X = Ga, In) compounds belong to a group of I–III–VI_2 (I = Cu, Ag; III = Al, Ga, In; and VI = S, Se, Te) chalcopyrite semiconductors with analogue zinc-blende lattices. Their thermoelectric properties have been investigated in both experiment and theory. In experiment, Plirdpring *et al.*[3] showed that the ZT value of polycrystalline bulk chalcopyrite $CuGaTe_2$ can reach 1.4 at high temperatures above 800 K. Liu *et al.*[4] successfully synthesized polycrystalline chalcopyrite compound $CuInTe_2$ and found that the ZT value of $CuInTe_2$ reached 1.18 at 850 K. Later on, Li *et al.*[5] synthesized the solid solutions $CuGa_{1-x}In_xTe_2$ ($x = 0$–1) by the isoelectronic substitution of element In (Ga) for Ga (In) in $CuGa(In)Te_2$ and investigated their thermoelectric properties from 300 K to 700 K. They found that the structure upon substitution provided a much higher Seebeck coefficient S and a relatively low thermal conductivity κ, so that the ZT value of the compound $CuGa_{0.36}In_{0.64}Te_2$ reached 0.91 at 701 K, nearly doubled in comparison to the ones of the mother compounds $CuGaTe_2$ and $CuInTe_2$. Doping is one of the most effective ways to enhance the thermoelectric performance.[6,7] It has been reported that the Seebeck coefficient can be effectively enhanced by the partial substitution of Ga by Sb in $CuGaTe_2$[8] and by doing Mn in $AgSbTe_2$.[9]

In a theoretical context, Parker *et al.*[10] researched the thermoelectric properties of $AgGaTe_2$ and related chalcopyrite structure materials using first-principles calculations. The doping and temperature dependences of the thermoelectric properties of $AgGaTe_2$[11] and $CuGaTe_2$[12] have also been discussed by using the density functional theory (DFT). However, the theoretical investigation on the electronic structures and the thermoelectric performance of $CuGa_{1-x}In_xTe_2$ is rare and incomprehensive. We also find that there exists a discrepancy between Refs. [13] and [5] on the measured electronic conductivities of solid solutions $CuGa_{1-x}In_xTe_2$. In Ref. [13], the conductivity σ showed a metallic behavior, namely, the electronic conductivity decreased with increasing temperature. While in Ref. [5], the electrical conductivity σ of four investigated samples increased rapidly when the temperature was above certain values, indicating a semiconductor property. In order to understand their electronic properties, in this paper, we investigate the structural and the electronic properties of the $CuGa_{1-x}In_xTe_2$ system as a function of the In composition based on the full-potential linearized augmented plane wave (FPLAPW) method.

*Project supported by the China Postdoctoral Science Foundation (Grant No. 2012M511603).

†Corresponding author. E-mail: d201177035@hust.edu.cn

© 2014 Chinese Physical Society and IOP Publishing Ltd

The organization of this paper is as follows. Section 2 gives details of the computational methods. Results and discussion concerning the structural, electronic, and thermoelectric transport properties of $CuGa_{1-x}In_xTe_2$ are presented in Section 3. Section 4 summarizes with a brief conclusion.

2. Computational details

The electronic structure calculations are performed via the full-potential all-electron linearized augmented plane wave (FP-LAPW) method implemented in the WIEN2K code.[14] The generalized gradient approximation of Perdew, Burke, and Ernzerhof[15] (GGA-PBE) is employed to relax the lattice constants and the atoms' positions. Convergence tests show that the use of 1000 k points in the irreducible Brillouin zone (IBZ) for the $CuGa_{1-x}In_xTe_2$ system is sufficient. The well converged basis sets with $R_{mt}K_{max} = 8.5$ are used, where R_{mt} and K_{max} are the smallest muffin-tin (MT) radius and the maximum size of the reciprocal-lattice vectors, respectively. The MT sphere radii for Cu, Ga, In, and Te ions are 2.5 a.u., 2.5 a.u., 2.5 a.u., and 2.06 a.u., respectively. We make the expansion up to $l = 10$ in the muffin tins. In all calculations, the tolerance of the total energy in self-consistency is less than 0.1 mRy per formula unit.

The transport properties are calculated by using the Boltzmann theory and the rigid band approach. The BoltzTraP code[16] with the constant scattering time approximation (CSTA) is used. A non-shifted mesh with 24000 k points is used for the transport calculations. The electronic transport quantities S, σ, and κ depend on the band structures, however the first-principle methods often underestimate the energy band gap significantly. To overcome the problem, here we employ a modified version of the exchange potential proposed by Becke and Johnson, known as the modified Becke Johnson (mBJ) potential,[17] which can give a much more accurate band gap than the standard LDA and GGA. The first-principles calcualtions, as a kind of theoritical method, have successfully described the electronic structures and the thermoelectric properties of many materials.[18–20]

3. Results and discussion

3.1. Crystal lattice and electronic structures

The crystal structure of $CuXTe_2$ (X = Ga, In) is the same as that of other ternary chalcopyrite with $I\bar{4}2d$ (group 122) symmetry, where Cu atoms occupy the 4a (0 0 0) site, X atoms occupy the 4b (0 0 1/2) site, and the Te atoms occupy the 8d (u 1/4 1/8) site. Thus, in order to completely describe the structure, three parameters need to be determined: the unit cell parameters a, c and the coordinate of the Te atoms u. If u is 1/4, the chalcopyrite type will have an ideal tetrahedral structure. However, experiments[3,5,21] show that the ternary chalcopyrite has tetragonal distortions, namely, u is not equal to 1/4, and the ratio $\eta = c/2a$ deviates from 1. A full relaxation is carried out to determine the lattice parameters a, c and the internal coordinate u. We use the experimental values as the initial lattice constants, i.e., $a = 6.024$ Å and $c = 11.924$ Å for $CuGaTe_2$.[22] The solid solutions $CuGa_{1-x}In_xTe_2$ are modeled in a conventional cell (containing four Cu atoms, four Ga/In atoms, and eight Te atoms) by isoelectronic substitution. The crystal structures of $CuGa_{1-x}In_xTe_2$ are shown in Fig. 1. Both calculated equilibrium lattice constants and lattice distortion parameter $\eta = c/2a$ are listed in Table 1, together with the available experimental data.

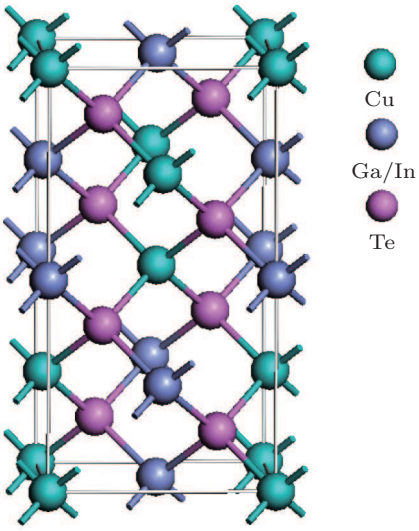


Fig. 1. (color online) Crystal structure of chalcopyrite compounds $CuGa_{1-x}In_xTe_2$.

Table 1. Calculated lattice parameters a, c and lattice distortion parameter $c/2a$ compared to the experimental results of solid solutions $CuGa_{1-x}In_xTe_2$.

x	a/Å	c/Å	$c/2a$
0	6.1125	12.2095	0.9987
	6.025[a]	11.948[a]	0.9915[a]
	6.021[b]	11.937[b]	0.9913[b]
	6.002[c]	11.949[c]	0.9954[c]
	6.024[d]	11.924[d]	1.0134[d]
	6.025[e]	11.935[e]	0.9905[e]
0.25	6.1568	12.3276	1.0011
	6.058[e]	12.068[e]	0.996[e]
0.5	6.2077	12.4403	1.002
	6.107[b]	12.177[b]	0.997[b]
	6.098[e]	12.196[e]	1[e]
0.75	6.2570	12.5717	1.0046
	6.147[e]	12.295[e]	1.0001[e]
1	6.3113	12.6730	1.004
	6.194[a]	12.416[a]	1.0023[a]
	6.195[b]	12.48[b]	1.0073[b]
	6.201[e]	12.379[e]	0.9981[e]
	6.1847[f]	12.4[f]	1.0025[f]

[a] Ref. [23]; [b] Ref. [24]; [c] Ref. [25]; [d] Ref. [22]; [e] Ref. [26]; [f] Ref. [27].

The calculated equilibrium parameters of solid solutions $CuGa_{1-x}In_xTe_2$ are slightly larger than the experimental val-

ues. This is because the GGA often overestimates the lattice constants of compounds. The deviations of the optimized lattice constants of $CuGaTe_2$ ($a = 6.1125$ Å) and $CuInTe_2$ ($a = 6.194$ Å) with the experimental values are within 1.9%, which indicates that our optimized results are reliable. It is observed from Table 1 that the calculated lattice parameters increase with the increase of In. Because the size of the substitution atom In is larger than that of Ga. The dependences of both lattice constants of solid solutions $CuGa_{1-x}In_xTe_2$ on In content x can be linearly fitted as follow:

$$a = 6.1095 + 0.1991x, \quad c = 12.2102 + 0.4684x. \qquad (1)$$

They are slightly different from the ones reported by León *et al.*[25]

$$a = 6.022 + 0.1625x, \quad c = 11.9495 + 0.4506x;$$

and by Gaburici *et al.*[28]

$$a = 6.015 + 0.168x, \quad c = 12.035 + 0.322x.$$

In order to have a better understanding of the electronic structures of $CuGa_{1-x}In_xTe_2$, the calculated band structures for a series of solid solutions with GGA and mBJ-GGA are investigated and shown in Fig. 2. As can be seen, they are direct gap semiconductors. The valence-band maximum (VBM) and the conduction-band minimum (CBM) are located at the Γ point. The isoelectronic substitution has no significant impact on the VBM. Since the valence bands primarily come from the hybridization of the Cu 3d and Te 5p orbitals, Ga and In atoms contribute very little to the VBM, while Ga/In and Te mainly contribute to the CBM. Due to the increases of the lattice constants with increasing In content, we find that the average distance $d_{\mathrm{III-Te}}$ ($d_{\mathrm{III-Te}} = (1-x)d_{\mathrm{Ga-Te}} + xd_{\mathrm{In-Te}}$) is elongated, whereas the average distance between Cu and Te is only slightly increased. The rate of alteration of $d_{\mathrm{III-Te}}$ is always larger than that of $d_{\mathrm{Cu-Te}}$ for solid solutions $CuGa_{1-x}In_xTe_2$. These structural variations induce band gap variations. The general trend has been summarized by Jaffe and Zunger.[29] The CBM is lowered as the bond contributing the most to it is stretched. The VBM is raised as the bond contributing the most to it is compressed. If the proposal above does work in the present investigated system, we should expect a dominant decrease of the CBM and therefore a band gap narrowing with increasing In content.

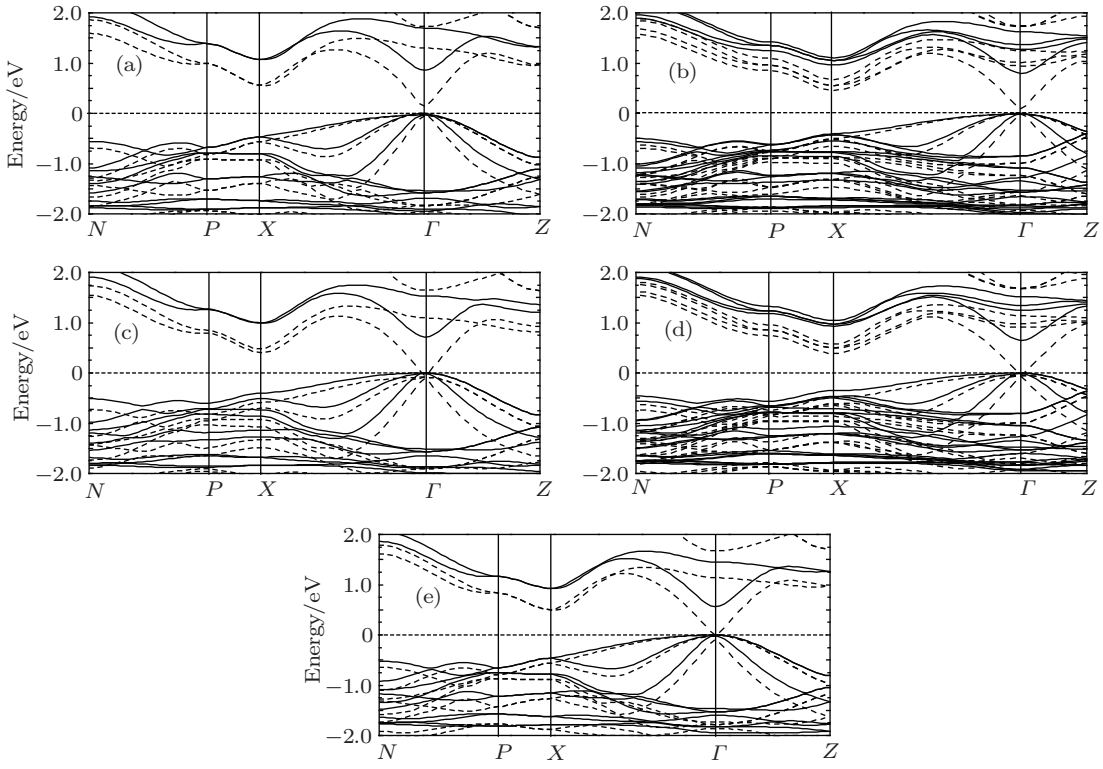


Fig. 2. Calculated band structures of solid solutions $CuGa_{1-x}In_xTe_2$ ((a) $x = 0$, (b) $x = 0.25$, (c) $x = 0.5$, (d) $x = 0.75$, (e) $x = 1$) with mBJ-GGA (solid lines) and GGA (dash lines) potentials.

The calculated band gaps of solid solutions $CuGa_{1-x}In_xTe_2$ with GGA and mBJ-GGA potentials are listed in Table 2, as well as the available experimental results and theoretical values. The GGA not only underestimates the band gap of $CuGaTe_2$, but also incorrectly predicts $CuInTe_2$ to be a metal. While the mBJ potential gives much improved band gap values of 0.73 eV and 0.56 eV for $CuGaTe_2$ and $CuInTe_2$, respectively. The band gap of $CuGaTe_2$ computed

with mBJ-GGA is 0.86 eV, which still remains smaller than the experimental value 1.24 eV. The major reason for this is the larger equilibrium volume discussed above. If evaluating at the experimental equilibrium volume, the band gap of $CuGaTe_2$ is 1.23 eV, which is in considerably better agreement with the experimental value. The calculated band gaps of solid solutions $CuGa_{1-x}In_xTe_2$ with the mBJ-GGA potential can be linearly fitted as follows:

$$E_g = 0.868 - 0.3x. \quad (2)$$

The band gap decreases with the increase of the In content.

Table 2. Calculated band gaps (in units of eV) together with experimental and other theoretical band gaps of solid solutions $CuGa_{1-x}In_xTe_2$.

x	This work		Exp.[a]	Exp.[b]	Cal.[c]	Cal.[d]
	GGA	mBJ-GGA				
0	0.13	0.86	0.9517	1.23	0.43	0.088
0.25	0.092	0.80				
0.5	0.033	0.72				
0.75	0	0.65				
1	0	0.56	0.7781	1.06	0.18	0

[a]Ref. [5]; [b]Ref. [22]; [c]Ref. [30]; [d]Ref. [31].

3.2. Transport properties

Based on the band structures calculated with the mBJ-GGA potential, the anisotropic transport properties of solid solutions $CuGa_{1-x}In_xTe_2$ are investigated. The calculated transport coefficients S and $S^2\sigma/\tau$ of $CuGaTe_2$ as a function of the carrier concentration at various temperatures are shown in Fig. 3. The values of S are positive at the considered temperatures, indicating that $CuGaTe_2$ is a p-type conductor and the majority carrier is the hole, which is consistent with the previous results. The Seebeck coefficients S for $CuGaTe_2$ first increase and then decrease with increasing temperature at low carrier concentrations, which is accordance with the experimental results.[3–5] Although the calculated Seebeck coefficients are qualitatively consistent with the experimental results, they fail quantitatively to a certain extent. For example, the Seebeck coefficients S of $CuGaTe_2$ with $p = 1.1 \times 10^{-24}$ m^{-3} at 300 K are 552 μV/K and 546 μV/K for xx and zz directions, respectively, which are larger than the experimental data 380 μV/K.[3] Such differences can be explained by the fact that Cu precipitates out of the matrix $CuGaTe_2$ at high temperatures, leading to a higher p-type carrier concentration.[3] The increase of the carrier concentration decreases the Seebeck coefficient, since the Seebeck coefficient and the carrier concentration of a degenerate semiconductor obey the following relationship:

$$S = \frac{8\pi^2 k_B^2 T}{3eh^2} m_d^* \left(\frac{\pi}{3n}\right)^{2/3}, \quad (3)$$

where m_d^* is the effective mass of the carrier. The variation trend of $S(T)$ for $CuGaTe_2$ is not the same as the theoretical result reported by Zou *et al.*,[12] where the Seebeck coefficient S increases with the increase of temperature over the whole considered concentrations. This discrepancy lies in that Zou *et al.* employed a GGA potential to investigate the transport properties, while we use the mBJ-GGA potential. From the above calculated band structures, it can be found that the mBJ-GGA potential not only improves the band gap values of $CuGa_{1-x}In_xTe_2$, but also has some effect on the valence band effective masses. Both are very important for the calculation of the transport properties. In addition, it can be seen from Fig. 3 that there is very little anisotropy outside the bipolar regime, the transport properties along the xx direction are very close to those along the zz direction.

Figure 3(b) shows the calculated $S^2\sigma/\tau$ as a function of doping and temperature for $CuGaTe_2$. Outside the bipolar regime, $S^2\sigma/\tau$ increases with increasing temperature due to the increase of the Seebeck coefficient S. The concentration dependence of $S^2\sigma/\tau$ at the given temperature can also be seen from Fig. 3. With increasing concentration, the magnitude of $S^2\sigma/\tau$ slowly increases, reaches a maximum, and then decreases. The peak values suggest that the thermoelectric performance of $CuGaTe_2$ can be optimized by appropriate doping.

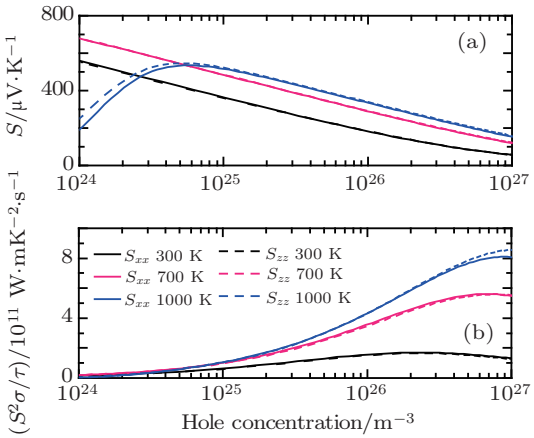


Fig. 3. (color online) Calculated (a) Seebeck coefficients S and (b) power factor divided by scattering time $S^2\sigma/\tau$ of $CuGaTe_2$ as a function of doping at various temperatures.

In order to understand the affect of the substitution of In in $CuGaTe_2$, the values of S and $S^2\sigma/\tau$, for 5 composition cases ($x = 0.0, 0.25, 0.5, 0.75, 1.0$) at 700 K and 1000 K, as a function of the carrier concentration are plotted in Figs. 4 and 5, respectively. The values of S and $S^2\sigma/\tau$ for the zz direction are respectively similar to those for the xx direction. Thus we only present the values of S and $S^2\sigma/\tau$ for the xx direction here. It can be seen that with increasing temperature and In content, the bipolar effect is more obvious. It results from that that the band gaps of solid solutions $CuGa_{1-x}In_xTe_2$

decrease with In fraction x increasing. When the temperature increases up to 1000 K, the bipolar effects in all solid solutions $CuGa_{1-x}In_xTe_2$ are much clearer. The Seebeck coefficient increases at low carrier concentrations, and after reaching a maximum value, it decreases with a further increase in the carrier concentration. The maximum Seebeck coefficient is denoted by $S_{max}(x)$, and the corresponding carrier concentration is represented by $n(S_{max})$.

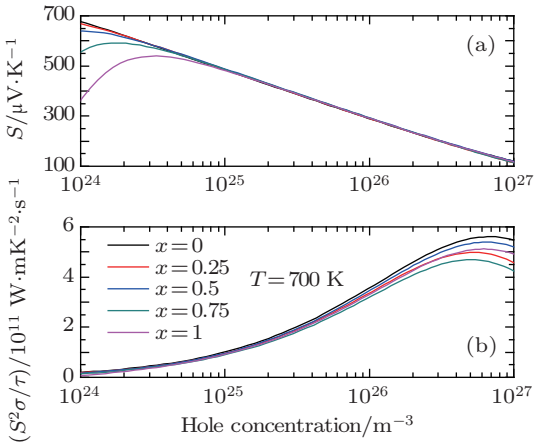


Fig. 4. (color online) Calculated (a) S and (b) $S^2\sigma/\tau$ of $CuGa_{1-x}In_xTe_2$ for the xx direction as a function of the carrier concentration at 700 K.

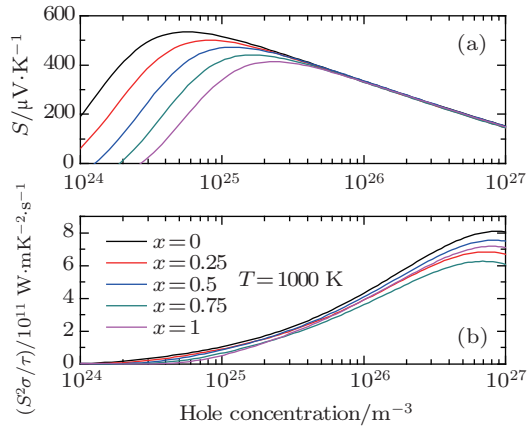


Fig. 5. (color online) Calculated (a) S and (b) $S^2\sigma/\tau$ of $CuGa_{1-x}In_xTe_2$ for the xx direction as a function of the carrier concentration at 1000 K.

The effects of the substitution on $S_{max}(x)$ and $n(S_{max})$ are shown for three given temperature cases (T = 300 K, 700 K, 1000 K) in Fig. 6. The $S_{max}(x)$ decreases linearly with increasing In fraction for all cases. The linear reduction of $S_{max}(x)$ for solid solutions is due to a linear reduction in their energy band gaps. At room temperature, it is found that $n(S_{max})$ has a weak dependence on the composition. This is because of the narrower width of the carrier distribution at lower temperatures and the insignificant variation of the density of states (DOS) in $CuGa_{1-x}In_xTe_2$ near the Fermi energy. However, $n(S_{max})$ increases rapidly with the increase of the composition at higher temperatures. Hossain *et al.*[32] have presented a detailed explanation based on the equations for the transport coefficients. The gradient of the Fermi–Dirac distribution broadens at higher temperatures. Therefore, it couples with more electronic states and has a closer relationship with the compositional variation, because the material variation has a substantial impact on the deeper conduction electronic states. Thus, this coupling shifts $n(S_{max})$ toward a higher concentration.

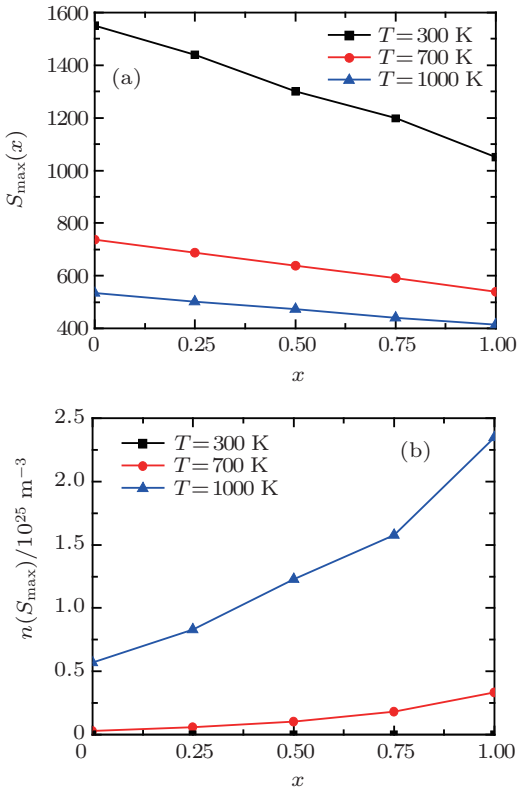


Fig. 6. (color online) The effects of the substitution on (a) $S_{max}(x)$ and (b) $n(S_{max})$ for three given temperature cases.

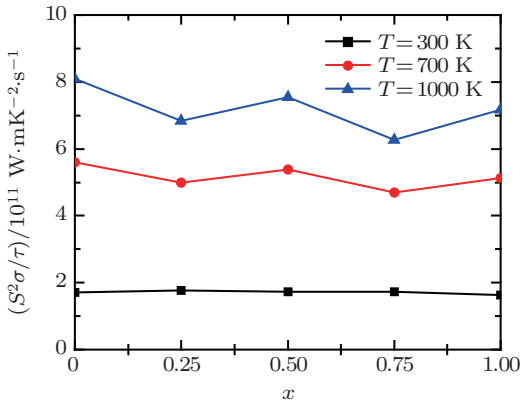


Fig. 7. (color online) The effect of the substitution on the maximum thermoelectric power $S^2\sigma/\tau$ for three given temperature cases.

The compositional variation of the maximum thermoelectric power at various temperatures is shown in Fig. 7. At room temperature, the maximum thermoelectric power has a weak dependence on the composition. While at high temperatures, the maximum thermoelectric power first decreases

with In concentration increasing, then increases, and finally decreases to a minimum value at $x = 0.75$. Based on the calculated $S^2\sigma/\tau$, the optimal doping concentrations for solid solutions $CuGa_{1-x}In_xTe_2$ are estimated to be in the range from 2.0×10^{26} m^{-3} to 9.0×10^{26} m^{-3}.

4. Conclusion

In summary, we have systematically investigated the electronic structures and thermoelectric properties of solid solutions $CuGa_{1-x}In_xTe_2$ via the full-potential linearized augmented plane-wave method and the semi-classical Boltzmann theory. It is shown that the calculated lattice parameters increase almost linearly with increasing In content. Compounds $CuGa_{1-x}In_xTe_2$ are all direct gap semiconductors. The band gap decreases linearly with the increase of the In content. The obtained Seebeck coefficients of $CuGaTe_2$ are in reasonable agreement with the experimental results. The majority carrier is the hole. With increasing temperature at low carrier concentrations, the Seebeck coefficient S first increases to the maximum Seebeck coefficient S_{max} and then decreases. When Ga is replaced by In, the maximum Seebeck coefficient linearly decreases and the bipolar effect of Seebeck coefficient S becomes more obvious as the In content increases. It results from the decrease of the band gap. Based on the calculated $S^2\sigma/\tau$ as a function of the carrier concentration, we estimate the optimal doping concentrations to be in the range from 2.0×10^{26} m^{-3} to 9.0×10^{26} m^{-3}, which can offer useful guidelines to improve the thermoelectric performance of $CuGa_{1-x}In_xTe_2$.

References

[1] Snyder G J and Toberer E S 2008 *Nat. Mater.* **7** 105

[2] Hochbaum A I, Chen R, Delgado R D, Liang W, Garnett E C, Najarian M, Majumdar A and Yang P 2008 *Nature* **451** 10

[3] Plirdpring T, Kurosaki K, Kosuga A, Day T, Firdosy S, Ravi V, Snyder G J, Harnwunggmoung A, Sugahara T, O-hishi Y, Muta H and Yamanaka S 2012 *Adv. Mater.* **24** 3622

[4] Liu R H, Xi L L, Liu H L, Shi X, Zhang W Q and Chen L D 2012 *Chem. Commun.* **48** 3818

[5] Li Y P, Meng Q S, Deng Y, Zhou H, Gao Y L, Li Y Y, Yang J F and Cui J L 2012 *Appl. Phys. Lett.* **100** 231903

[6] Liu Y, Li H J, Zhang Q, Li Y and Liu H T 2013 *Chin. Phys. B* **22** 057201

[7] Yang M J, Shen Q and Zhang L M 2011 *Chin. Phys. B* **20** 106202

[8] Cui J, Li Y, Du Z, Meng Q and Zhou H 2013 *J. Mater. Chem. A* **1** 677

[9] Zhang H, Luo J, Zhu H T, Liu Q L, Liang J K, Li J B and Liu G Y 2012 *Chin. Phys. B* **21** 106101

[10] Parker D and Singh D 2012 *Phys. Rev. B* **85** 125209

[11] Wu W, Wu K, Ma Z and Sa R 2012 *Chem. Phys. Lett.* **537** 62

[12] Zou D F, Xie S H, Liu Y Y, Lin J G and Li J Y 2013 *J. Alloys Comp.* **570** 150

[13] Kuhn B, Kaefer W, Fess K, Friemelt K, Turner Ch, Wendl M and Bucher E 1997 *phys. Stat. Sol. (a)* **162** 661

[14] Blaha P, Schwarz K, Madsen G, Kvasnicka D and Luitz J 2001*WIEN2K, An Augmented Plane Wave+Local Orbitals Pro-gram for Calculating Crystal Properties* (K Schwarz, Tech. Univ. Wien, Austria)

[15] Perdew J P, Burke K and Ernzerhof M 1996 *Phys. Rev. Lett.* **77** 3865

[16] Madsen G K H and Singh D J 2006 *Comput. Phys. Commun.* **175** 67

[17] Becke A D and Johnson E R 2006 *J. Chem. Phys.* **124** 221101

[18] Pan Z J, Zhang L T and Wu J S 2005 *Acta Phys. Sin.* **54** 5308 (in Chinese)

[19] Feng J, Xiao B and Chen J C 2007 *Acta Phys. Sin.* **56** 5990 (in Chinese)

[20] Peng H, Wang C L, Li J C, Zhang R Z, Wang H C and Sun Y 2011 *Chin. Phys. B* **20** 046103

[21] León M, Merino J M and Martin De Vidales J L 1992 *J. Mater. Sci.* **27** 4495

[22] Bodnar I V and Orlova N S 1986 *Cryst. Res. Technol.* **21** 1091

[23] Abrahams S C and Bernstein J L 1973 *J. Chem. Phys.* **59** 5415

[24] Grzeta-Plenkovic B and Santic J 1983 *J. Appl. Cryst.* **16** 576

[25] León M, Merino J M and MartiN De Vidales J L 1993 *J. Vac. Technol. A* **11** 2430

[26] Avon J E, Yoodee K and Woolley J C 1984 *J. Appl. Phys.* **55** 524

[27] Knight K S 1992 *Mater. Res. Bull.* **27** 161

[28] Gaburici D, Lazarescu M F, Manea A and Sandu V 2000 *Cryst. Res. Technol.* **35** 265

[29] Jaffe J E and Zunger A 1984 *Phys. Rev. B* **29** 1882

[30] Rashkeev S N and Lambrecht W R L 2001 *Phys. Rev. B* **63** 16521

[31] Zhang X Z, Shen K S, Jiao Z Y and Huang X F 2013 *Comput. Theor. Chem.* **1010** 67

[32] Hossain M Z and Johnson H T 2012 *Appl. Phys. Lett.* **100** 253901